



Published in final edited form as:

Exp Lung Res. 2007 ; 33(3-4): 169–183. doi:10.1080/01902140701364458.

A MicroCT-Based Method for the Measurement of Pulmonary Compliance in Healthy and Bleomycin-Exposed Mice

Scott Shofer, MD, PhD¹, Cristian Badea, PhD², Scott Auerbach, PhD³, David A. Schwartz, MD³, and G. Allan Johnson, PhD²

¹*Pulmonary, Allergy, and Critical Care, Duke University Medical Center, Durham, NC*

²*Center for In Vivo Microscopy, Radiology, Duke University Medical Center, Durham, NC*

³*National Institute of Environmental Health Sciences, Research Triangle Park, NC*

Abstract

Micro-computed tomography (microCT) is being increasingly used to examine small animal models of pulmonary injury. We have developed a microCT technique suitable for the determination of pulmonary compliance in injured mice. Lung volumes in normal mice were radiographically determined at end-inspiration and end-expiration and pulmonary compliance was calculated at two timepoints 2 weeks apart, while a second group of mice were given bleomycin and imaged 3 weeks following drug administration. Compliance measurements were validated using a commercially available ventilator system. MicroCT pulmonary compliance measurements are suitable for longitudinal measurements, and correlate with physiologic measurements of pulmonary compliance.

Keywords

MicroCT; pulmonary compliance; pulmonary fibrosis

INTRODUCTION

Micro-computed tomography (microCT) is an increasingly used technique for imaging small animal models of pulmonary disease^{19, 17, 2, 21}. These studies provide minimally invasive, longitudinal observations of in vivo pathological changes associated with a variety of pulmonary disease models. As these studies become more common, a need exists for standard physiologic measurements in conjunction with imaging. This will integrate imaging-based information with the effects of anatomical perturbations, as measured by microCT imaging. The majority of previous studies that have combined physiologic measurements with imaging have been performed in large animals and have focused on regional motion of lung volumes²¹. Few studies have applied CT techniques to mice. Mitzner measured lung volumes and changes in functional reserve capacity with age in anesthetized mice⁸, while Postnov examined lung volumes in emphysematous mice and was able to quantify severity of emphysema based on changes in lung density measured in Hounsfield units (HU)¹⁵. Recently, microCT measurements of pulmonary compliance were made in normal mice and rats using breath-holding at various pressures and calculating lung volumes from the corresponding images to produce a pressure-volume curve⁸. Unfortunately, no correlation to standard measurements were performed in this study.

The objective of this current study was to develop a microCT-based method to measure pulmonary compliance in mice, which would be suitable for repeated measurements in the same animal over time, would be rapidly performed to permit imaging of multiple animals on a given day, and would minimize the exposure to ionizing radiation. We have developed an *in vivo* technique suitable for mice, which permits measurement of dynamic pulmonary compliance longitudinally in time. The procedure can be performed in approximately 15 minutes by applying respiratory gating during imaging. To validate our measurements and establish the sensitivity of the technique, we performed compliance measurements in normal and bleomycin-exposed mice and compared CT-derived compliance measurements with quasi-static compliance measurements using a commercially available small animal ventilator. Normal mice were serially imaged to demonstrate the application of this technique to longitudinal studies, while bleomycin-exposed mice were studied to demonstrate the applicability of this technique to investigate commonly used pulmonary models of fibrosis. This study also assessed the sensitivity of the technique to changes in key parameters in pulmonary physiology.

METHODS AND MATERIALS

Experimental Design

All experimental procedures conformed to National Research Council guidelines and were approved by the Duke University Institutional Animal Care and Use Committee. Five pathogen-free male C57BL/6 mice (Charles River Labs, Wilmington, MA) weighing 29.1 ± 3.1 g (mean \pm SD) at the time of initial saline aspiration were kept in a pathogen-free vivarium and fed food and water *ad libitum*. The mice were sedated with isoflurane, hung on a specially designed instillation board at 70° by their front incisors with the tongue retracted, and instilled with 50 μ l of sterile normal saline in the retropharyngeal space to induce aspiration.⁷ Animals were allowed to recover and were then imaged by microCT at one week and three weeks following instillation, as previously described.²

A second group of 10 pathogen-free female 129S6/SvEvTac mice (Taconic Labs, Hudson, NY) weighing 19.5 ± 1.1 g were treated with retropharyngeal aspiration of 50 μ l of sterile saline or increasing doses of bleomycin (Mayne Pharma Inc., Paramus, NJ) dissolved in sterile saline (2.0, to 3.5 U/kg body weight in 0.5 U increments) in groups of two at each bleomycin dose. Mice were then housed in a pathogen-free vivarium, fed, and watered *ad libitum*. MicroCT compliance (Cct) measurements were performed at a single timepoint 3 weeks following bleomycin aspiration. Following imaging, all animals were recovered. Quasi-static compliance (Cqs) measurements were performed on the day following imaging, as described in the next section.

Animal Preparation of MicroCT Imaging

Mice were imaged as previously described.² Animals were sedated with isoflurane and intraperitoneally (ip) injected with ketamine (75 mg/kg) and xylazine (11 mg/kg) to achieve prolonged sedation. The animals were then perorally intubated with a 22ga Jelco[®] IV catheter trimmed to 2.1 cm (Medex Medical Ltd, Lancashire, UK) using a modification of the procedure described by Brown.⁵ Mice were placed in a plexiglass cradle and suspended vertically for imaging. Sedation was maintained with isoflurane 2.5% administered via a custom-built mechanical ventilator.^{10,11} ECG was monitored by placement of electrodes on the animal's footpads, and body temperature was maintained using a rectal thermistor controlling heating lamps placed around the mouse. Ventilation was provided via a constant-pressure ventilator at a respiratory rate of 120 breaths per minute and 30% inspired O₂. Inspiratory pressure was adjusted to 8 cm H₂O using a water manometer. Inspiratory time was set to 24% (0.120 s) of the breath cycle with opening of the ventilator expiratory valve occurring at 0.130 s and

remaining open until the initiation of the next breath. This breath cycle resulted in positive end-expiratory pressures (PEEP) of 4 cm H₂O. Ventilator air pressures were checked at the beginning and end of imaging for each animal and adjusted as necessary. Following imaging, animals were recovered on a heating pad to maintain body temperature. Extubation occurred when the animal was spontaneously breathing and had recovery of pinch and righting reflexes. The oropharynx was carefully suctioned prior to removal of the endotracheal tube.

MicroCT Image Acquisition

MicroCT images were acquired on a custom system designed explicitly for cardiopulmonary imaging.² X-ray parameters were as follows: 80 kVp, 170 mA, and 12 ms exposure per projection. 380 projections were acquired at 0.5° increment between projections for a total rotation angle of 190°. Total imaging time was approximately 8 minutes per dataset. Two complete datasets at end-inspiration and end-expiration were collected for each mouse by prospective respiratory gating of the imaging system at 0.115 s and 0.370 s from the inspiratory ventilator trigger respectively, with a 0.010 s window for image acquisition. The 2D projection images were used to reconstruct tomograms by Feldkamp algorithm⁶ using a commercial software package (Cobra EXXIM, EXXIM Computing Corp., Livermore, CA). Data were reconstructed with Parker weighting¹⁴ as isotropic 512 × 512 × 512 arrays with effective digital sampling of 100 μm along all three axes.

Image Processing

Reconstructed images were converted to Hounsfield units (HU) by scaling air to -1000 HU and plexiglass (as a surrogate for water) to 0 HU using a conversion file written for MATLAB (The MathWorks, Natick, MA). Files were then imported to Image J <<http://rsb.info.nih.gov/ij/>> and cropped from the first rib to the tip of the right lower lobe. Images were modified to exclude tissue <500 HU, which excluded all tissue except for the ribs followed by application of a convex hull algorithm, which formed an elliptical space surrounding the outer aspect of the ribs and included the surface bounded by this ellipse. This procedure was performed for each slice in the axially-oriented image stacks and was used as a mask to digitally exclude all tissue outside of the bounded space. The resulting thoracic images included all of the trachea below the first rib, all of the intrathoracic anatomical structures, and the cephalad portions of the liver, as well as a thin strip of intercostal tissues.

Lung tissue was digitally isolated from the remainder of the thoracic structures using the “connected threshold grower” shareware plugin for Image J that implements a segmentation technique named region growing (Add Reference : R. **Gonzales**, R. Woods **Digital Image Processing**, Addison-Wesley Publishing Company, 1992). Starting at a position in the trachea, images were adjusted by an iterative process so that only tissue within the lung parenchyma was included in the subsequent images (Fig. 1). In order to permit accurate separation of lung parenchyma from the soft tissue structures, the thresholding parameters were adjusted in such a way that the large vessels were excluded from the images derived through this process. Lung volume was determined by summation of the total number of voxels in the digitally isolated volume and multiplying by the voxel volume (100 μm³). This procedure was performed for each inspiratory and expiratory dataset.

Cavalieri Lung Volume Estimates

Injured pulmonary parenchyma develops a radiographic density similar to the adjacent intrathoracic structures (such as the heart and great vessels), which prevents an accurate and reproducible digital separation of the pulmonary structures. Segmentation of the injured lung images by hand is labor-intensive and time-consuming. To avoid these difficulties, we adapted a Cavalieri method volume estimation from standard morphometric techniques to make lung volume measurements from the digital images of the bleomycin-injured animals.¹⁴ Ten

random stratified sections were selected from each processed dataset, with initial section selected from a table of random numbers used only once. A series of digital crosses were applied to each section, with a point defined as the intersection of the lines of each cross. The cross-lines were a single pixel in thickness, forming a point 1 pixel square with a density of 200 pixel area/point (Fig. 2). Points overlying the thoracic cage and overlying the lung parenchyma were counted for each section. Lung volumes were determined as previously described and shown by Equation 1:¹⁴

$$V_{lu} = P_{lu} / P_{th} * V_{th} \quad (1)$$

Where V_{lu} is the calculated lung volume, P_{lu} is the total number of points overlying the lung parenchyma, P_{th} is the number of points overlying the entire thorax, and V_{th} is the volume of the thoracic cage measured by summation of the voxels in the thoracic cage multiplied by volume of the individual voxels. Points overlying visible vessels were excluded from pulmonary volume estimates because these were in the digitally-based lung volume measurements.

MicroCT-Based Compliance Measurements

Imaging-based compliance was calculated using Equation 2:¹

$$C = \Delta V / \Delta P \quad (2)$$

Where C is compliance, ΔV is end-inspiratory lung volume minus end-expiratory lung volume, and ΔP is end-inspiratory pressure minus end-expiratory pressure. In the cases where delivered airway pressure were different at the beginning and end of imaging, the mean value for the inspiratory and expiratory pressure was used to calculate ΔP .

Quasi-static Compliance Measurements

The day following imaging, quasi-static compliance measurements were performed using a computer-controlled small animal ventilator (flexiVent, SCIREQ, Scientific Respiratory Equipment, Montreal, Quebec, Canada). Mice were sedated with ip pentobarbital sodium (50 mg/kg) and tracheotomy was performed using p10 tubing, which was secured with two ligatures around the trachea, followed by paralysis with pancuronium -(0.8 mg/kg ip). Animals were ventilated at a respiratory rate of 120 breaths per minute and PEEP was set at 3 cm H₂O per recommended protocol from the manufacturer. Prior to quasi-static compliance measurements, the mouse lungs were inflated to total lung capacity using 30 cm H₂O pressure held for 3 seconds. Lungs were inflated from PEEP to 25 cm H₂O and back in 7 increments for inflation and deflation with a 3-second pause at each increment. Compliance was calculated using the software supplied with the ventilator from the slope of the Salazar-Knowles¹⁹ equation fit to the deflation limb of the pressure-volume curve. Animals were sacrificed with a lethal dose of pentobarbital, following compliance measurements.

Histology

After completion of quasi-static compliance measurements, the chest cavity was opened and the lungs were inflated with 10% phosphate-buffered formalin to 20 cm H₂O and held for 5 minutes. The trachea was tied off and the samples were placed in formalin for further fixation. Samples were then trimmed and the left lung was embedded in paraffin, 6 μ m coronal sections were taken from the midlung and stained with hematoxylin and eosin (H&E) or Masson's trichrome stain in adjacent sections.

Scoring of lung injury was performed using the Image-Pro Plus 5.1 software package (MediaCybernetics, Silver Spring, MD). A single, 6 μm -thick, coronal slice was obtained from the mid-left lung from each mouse and stained with trichrome. Each slide was then digitized using a SprintScan 4000 (Polaroid, Waltham, MA). A blinded observer (author SA) calculated the area occupied by total lung, large airways, large blood vessels and fibrous tissue using the trapezoidal tool for region of interest selection. To determine the percentage of fibrotic lung, the total affected area was divided by the complete area of the lung slice with the exception of the large airways and blood vessels, which were subtracted from the total area.

Statistics

Data are presented as mean and standard deviation. Analysis of variance was performed for mice treated with bleomycin, while paired t-test was performed for comparison of serial compliance measurements. All statistical calculations were performed using the statistics toolbox in MATLAB with significance defined as $p < 0.05$. Comparison of correlation between Cct and Cqs measurements was performed as described by Bland and Altman.³

RESULTS

MicroCT Imaging

Five C57BL/6 mice were imaged at the first timepoint and recovered following intubation; however, one animal suffered an injury of the upper extremity and was sacrificed per protocol. A second mouse expired 10 days after initial imaging of unknown cause. The remaining 3 mice were successfully imaged at week 3 and recovered for quasi-static compliance measurements. All 10 of the 129S6 mice were successfully imaged and recovered for quasi-static compliance measurements. All imaging for each group was conducted on the same day.

Compliance Measurements in Untreated C57BL/6 Mice

Inspiratory and expiratory lung volumes for weeks 1 and 3 are shown in Table 1. Cct, using computerized segmentation for lung volume determination, were 0.0829 ± 0.0077 ml/cm H_2O and 0.0856 ± 0.0279 ml/cm H_2O from week 1 to week 3 respectively, and were not statistically different from Cqs (Table 1, $p = 0.826$). No significant change was noted in compliance from week 1 to week 3 ($p = 0.50$). The mice did not develop any radiographic evidence of injury from repeated imaging, although there was a small weight loss (31.3 ± 1.01 g week 1 versus 29.7 ± 1.35 g week 3) between imaging intervals.

Comparison of Digital and Cavalieri Lung Volume Measurements

Cavalieri lung volume estimates were made on C57BL/6 mice for both inspiratory and expiratory datasets collected at the first imaging timepoint for the three animals that survived imaging. Estimates were performed for all 6 image datasets. Cavalieri lung volume estimates were within 2.3% of digital measurements, underestimating digitally derived volumes by 23.6 ± 47.0 μl .

Histologic Lung Injury Assessments in Bleomycin Exposed Mice

Fraction of lung injury due to fibrosis is presented in Table 3. Injury severity was highly variable and displayed no trends with increasing bleomycin dose. There was no statistical significance between groups.

Compliance Measurements in Bleomycin-Exposed Mice

Similar to histologic evidence of injury, lung injury on microCT images was variable between animals within exposure groups, Lung injury was primarily peribronchovascular in nature, but

was heterogenous regarding regions of the lung involved and the degree of severity of lung injury between animals (Fig. 3).

Inspiratory and expiratory lung volumes are shown in Table 2. Quasi-static compliance measurements displayed a trend towards lower values with increasing bleomycin dose, which was not statistically significant as measured by both microCT ($p = 0.464$) and quasi-static ($p = 0.599$) measurements (Fig. 4).

The overall variability in lung injury made it difficult to detect trends in changes of pulmonary compliance. However, the three animals with the most severe injury, as measured by histology and radiography, did display the lowest values of C_{qs} at 0.0582, 0.0547, and 0.0562 ml/cm H_2O , while C_{ct} values were 0.0738, 0.0740, and 0.0558 ml/cm H_2O for the same three animals, respectively (Fig. 3).

Bland-Altman Analysis

The mean difference in compliance measurements between microCT and conventional ventilation is -0.0024 ± 0.0130 ml/cm H_2O , which suggested a small and physiologically insignificant bias in the C_{ct} measurement (Fig. 5). No trend is evident in the distribution of differences in compliance measurements between the C57BL/6 mice and the 129S6 mice.

DISCUSSION

We have demonstrated a method of performing imaging-based compliance measurements in mice, which correlates well with a direct physiologic assessment of lung compliance. This technique is minimally invasive, which permits serial measurements in the same animal, while also providing anatomic information regarding the distribution and severity of lung injury in animals exposed to bleomycin (and likely to other agents which cause lung injury). As expected, there was no change in pulmonary compliance related to serial imaging of normal mice. In aggregate, these results indicate that microCT can be used serially to evaluate lung injury and that under certain circumstances these measures correlate with changes in lung compliance.

Preclinical imaging systems, such as microCT, magnetic resonance imaging, and positron emission tomography, are becoming more frequently employed for imaging the anatomic features associated with a wide variety of normal and abnormal pulmonary conditions.²¹ As studies using these imaging methods become more prevalent, correlation of conventional phenotypic measurements with new imaging data will provide better understanding of the alteration in the animals physiology associated with the visualized abnormalities. In the present study, we have measured C_{ct} in a group of C57BL6 mice two weeks apart showing stable compliance and good correlation with C_{qs} (Table 1). The PEEP applied between the C_{qs} and C_{ct} were different at 3 cm H_2O and 4 cm H_2O respectively, with consistent results between the two methods suggesting that the animals were being ventilated at the linear portion of the pressure-volume curve at both levels of PEEP. Compliance measurements are slightly above previously observed values due to larger size of the animals in the present study.¹⁷ Interestingly, inspiratory and expiratory lung volumes increased from week 1 to 3 without significant change in body weight, tidal volume, or compliance suggesting a possible component of air trapping that developed during the second set of studies. This air trapping may be due to inflammation related to repeated intubations, although previous studies with more frequent serial intubations did not show evidence of inflammation associated with this procedure.⁸ This change in lung volumes from week 1 to week 3 would not have been detected by measurement of C_{qs} alone because there was no trend in compliance measurements.

Expiratory lung volumes in both C57BL6 and 129S6 mice in this study are approximately 100 μ l larger than previously described by Mitzner¹³, which is likely due to the larger animal size, interstrain variation, and positive pressure ventilation used in this study¹⁷.

Bleomycin administration produced varying degrees of lung injury, which were more apparent on imaging (Fig 3) and histology, than by changes in compliance (Fig 4). The variation in lung injury is likely due to difficulty in performing reproducible retropharyngeal aspirations of bleomycin. Some mice developed coughing after administration of the bleomycin solution, while others appeared to swallow the drug and therefore had a milder resulting lung injury. Cqs did show a decline in 3 animals with the most severe injury by imaging and histology; however, Cct was not as sensitive as Cqs in these animals (Fig 3). Previous compliance measurements in rats exposed to bleomycin have been variable. Schlegle et al.²⁰ observed a decline in quasi-static compliance from 0.88 to 0.32 ml/cm H₂O in rats exposed to 0.5 U bleomycin, while Borzone⁴ showed no effect of bleomycin on pulmonary compliance, although these animals were assessed 120 days post-administration and so may have had regression of some of the initial fibrotic injury.

The radiographic findings associated with bleomycin exposure in this study are areas of peribronchial consolidation, primarily located in the upper and posterior lung zones. These areas appear to correlate with foci of fibrosis on the histologic specimens (Fig 3) as previously described.¹² Cqs measurements were decreased only in animals that developed areas of consolidation with density of greater than 250 HU (data not shown). The decrease in Cqs did not correlate with the amount of injured lung as demonstrated in panels Fig 3a-c where the amount of injury ranges from near total consolidation of the left lung with smaller areas of peribronchial injury on the right (Fig 3a) to scattered foci of consolidation primarily effecting the right lower lobe bronchus (Fig 3b), and a more diffuse pattern of injury (Fig 3c). Despite these gradations of injury, Cqs were essentially identical for the 3 animals (0.056 to 0.059 ml/cm H₂O). Cct were variable in this subgroup of mice (see text of Fig 3).

Bland-Altman analysis reveals small measurement bias of -0.0024 ml/cm H₂O between Cct and Cqs, with a standard deviation of \pm 0.0130. Assuming a normally distributed population, this analysis suggests that 95% of the difference between the two measurements should fall within a range of -0.0285 and 0.0237 ml/cm H₂O. Three likely sources of variation are associated with the Cct measurement. MicroCT compliance measurements require both an inspiratory and expiratory lung volume measurement, resulting in a doubling of the SD associated with each tidal volume determination. Previously performed serial measurements of lung volumes in individual animals at the same inflation resulted in a SD of \pm 27.0 μ l. Secondly, Cavalieri lung volume estimates underestimate digitally derived lung volumes by 23.6 ± 47.0 μ l, again, this error will be doubled for each tidal volume determination. Overall, this measurement error may result in a variation in tidal volume of up to 148.0 μ l for each Cct estimation. Finally, Cqs were performed the day following Cct measurements, which may have resulted in alterations in compliance due to unrecognized injury associated with the imaging procedure.

This procedure does have significant variation compared with the more accurate Cqs, however measurement of Cct permits determination of lung volume at the time compliance measurement which is not possible with Cqs. This is important as lung compliance varies with degree of inflation. In addition, being an imaging method, microCT permits the assessment of heterogeneity of ventilation within the injured lung at both end-inspiration and end-expiration.

In conclusion, we have described and validated a microCT-based method suitable for repeated measurements of pulmonary compliance in individual mice. This procedure provides both physiologic data on pulmonary compliance and detailed anatomic information regarding

location and severity of parenchymal pulmonary injury. This technique may have a wide variety of applications in future studies of pulmonary physiology in small animal models.

Acknowledgements

We wish to thank Dr. Steve Young and Dr. William M. Foster for their thoughtful review of this manuscript. In addition, Julie Boslego Mackel provided invaluable assistance with the animal handling, and Erin Potts assisted with the flexivent measurements. Work was performed at the Duke Center for In Vivo Microscopy, an NIH/NCRR Biomedical Technology Resource Center (P41 RR005959), and (ES011961), with additional funding provided by NCI (R24 CA092656).

REFERENCES

1. Agostoni, E.; Hyatt, RE. Handbook of Physiology. Am. Physiol. Soc.; Bethesda MD: 1986. Static behavior of the respiratory system.
2. Badaea C, Hedlund LW, Johnson GA. Micro-CT with respiratory and cardiac gating. *Med Phys* 2004;31:3324–3329. [PubMed: 15651615]
3. Bland JM, Altman DG. Statistical methods for assessing agreement between two methods of clinical measurement. *Lancet* 1986;327:307–310. [PubMed: 2868172]
4. Borzone G, Moreno R, Urrea R, et al. Bleomycin-induced chronic lung damage does not resemble human idiopathic pulmonary fibrosis. *Am J Respir Crit Care Med* 2001;163:1648–1653. [PubMed: 11401889]
5. Brown RH, Walter DM, Greenber RS, et al. A method of endotracheal intubation and pulmonary functional assessment for repeated studies in mice. *J Appl Physiol* 1999;87:2362–2365. [PubMed: 10601190]
6. Feldkamp LA, Davis LC, Kress JW. Practical cone-beam algorithm. *J. Opt Soc Am A* 1984;1:612–619.
7. Foster WM, Walters DM, Longphre M, et al. Methodology for the measurement of mucociliary function in the mouse by scintigraphy. *J Appl Physiol* 2001;90:1111–1118. [PubMed: 11181627]
8. Glaab T, Mitzner W, Braun A, et al. Repetitive measurements of pulmonary mechanics to inhaled cholinergic challenge in spontaneously breathing mice. *J Appl Physiol* 2004;97:1104–1111. [PubMed: 15121749]
9. Guerrero T, Castillo R, Sanders K, et al. Novel method to calculate pulmonary compliance images in rodents from computed tomography acquired at constant pressures. *Phys Med Biol* 2006;51:1101–1112. [PubMed: 16481680]
10. Hedlund LW, Cofer GP, Owen SJ, et al. MR-compatible ventilator for small animals: computer-controlled ventilation for proton and noble gas imaging. *Magn Reson Imaging* 2000;18:753–759. [PubMed: 10930785]
11. Hedlund LW, Johnson GA. Mechanical ventilation for imaging the small animal lung. *ILAR J* 2002;43:159–174. [PubMed: 12105383]
12. Hirose N, Lynch DA, Cherniack RM, et al. Correlation between high resolution computer tomography and tissue morphometry of the lung in bleomycin-induced pulmonary fibrosis in the rabbit. *Am Rev Respir Dis* 1993;147:730–738. [PubMed: 7680190]
13. Mitzner W, Brown R, Lee W. In vivo measurement of lung volumes in mice. *Physiol Genom* 2001;4:215–221.
14. Mouton, PR. Principles and practices of unbiased stereology, an introduction for bioscientists. The Johns Hopkins University Press; Baltimore, MD: 2002.
15. Parker DL. Optimal short scan convolution reconstruction for fan beam CT. *Med Phys* 1982;9:254–257. [PubMed: 7087912]
16. Postnov AA, Meurrens K, Weiler H, et al. In vivo assessment of emphysema in mice by high resolution x-ray microtomography. *J Micro* 2005;220:70–75.
17. Reinhard C, Eder G, Fuchs H, et al. Inbred strain variation in lung function. *Mammalian Genome* 2002;13:429–437. [PubMed: 12226708]

18. Ritman EL. Micro-computed tomography of the lungs and pulmonary-vascular system. *Proc Am Thorac Soc* 2005;2:477–480. [PubMed: 16352751]
19. Salazar E, Knowles JH. An analysis of pressure-volume characteristics of the lungs. *J Appl Physiol* 1964;19:97–104. [PubMed: 14104296]
20. Schelegle ES, Walby WF, Mansoor JK, et al. Lung vagal afferent activity in rats with bleomycin-induced lung fibrosis. *Resp Physiol* 2001;126:9–27.
21. Schuster DP, Kovacs A, Garbow J, et al. Recent advances in imaging the lungs of intact small animals. *Am J Respir Cell Mol Biol* 2004;30:129–138. [PubMed: 14729505]
22. Simon BA, Christensen GE, Low DA, et al. Computed tomography studies of lung mechanics. *Proc Am Thorac Soc* 2005;2:517–521. [PubMed: 16352757]

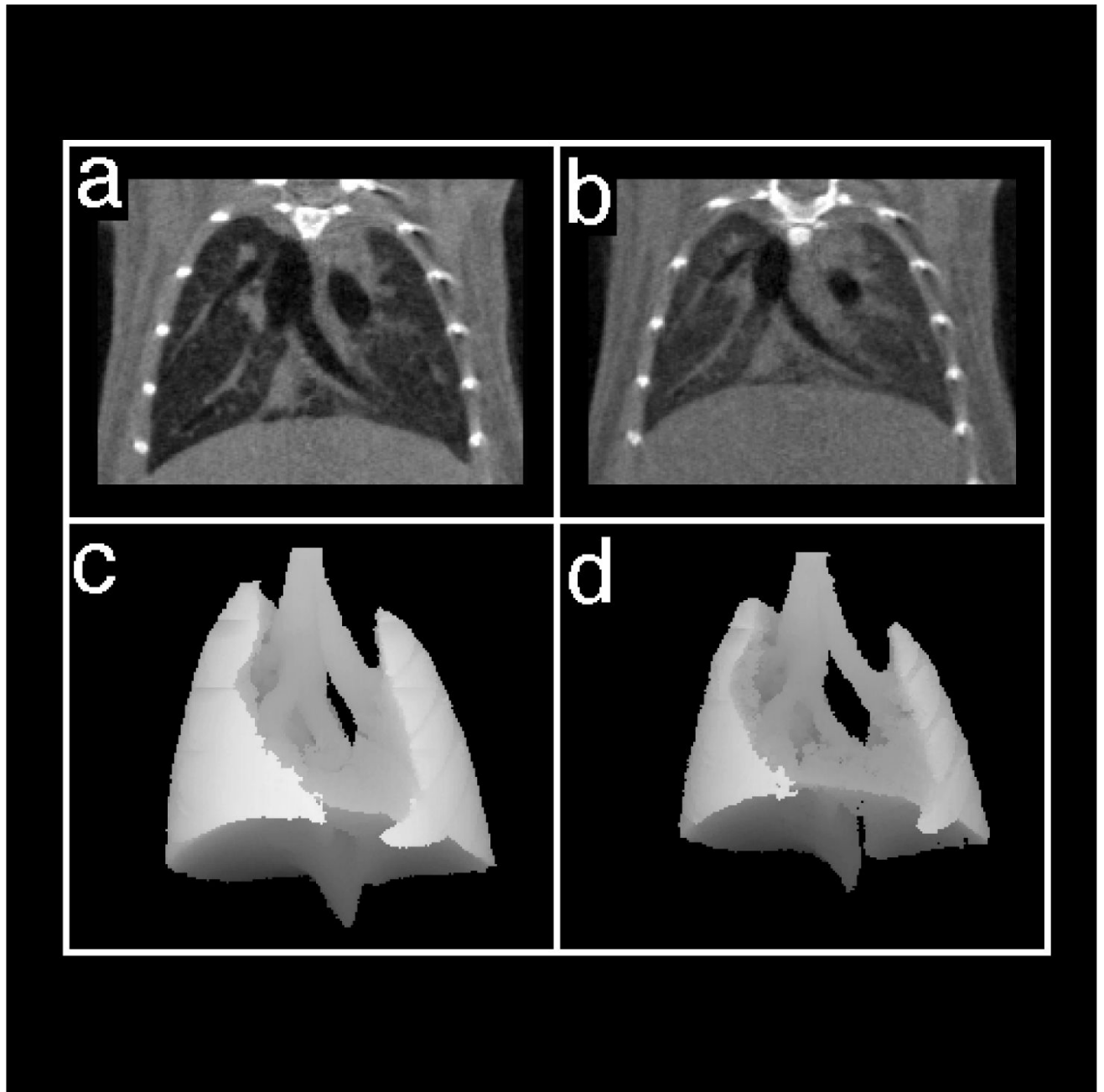


Figure 1. Coronal images of control mice at end-inspiration (a) and end-expiration (b). Three-dimensional mean intensity projections of end-inspiration (c) and end-expiration (d) were used to compute total lung volumes. Imaging parameters are described in the text.

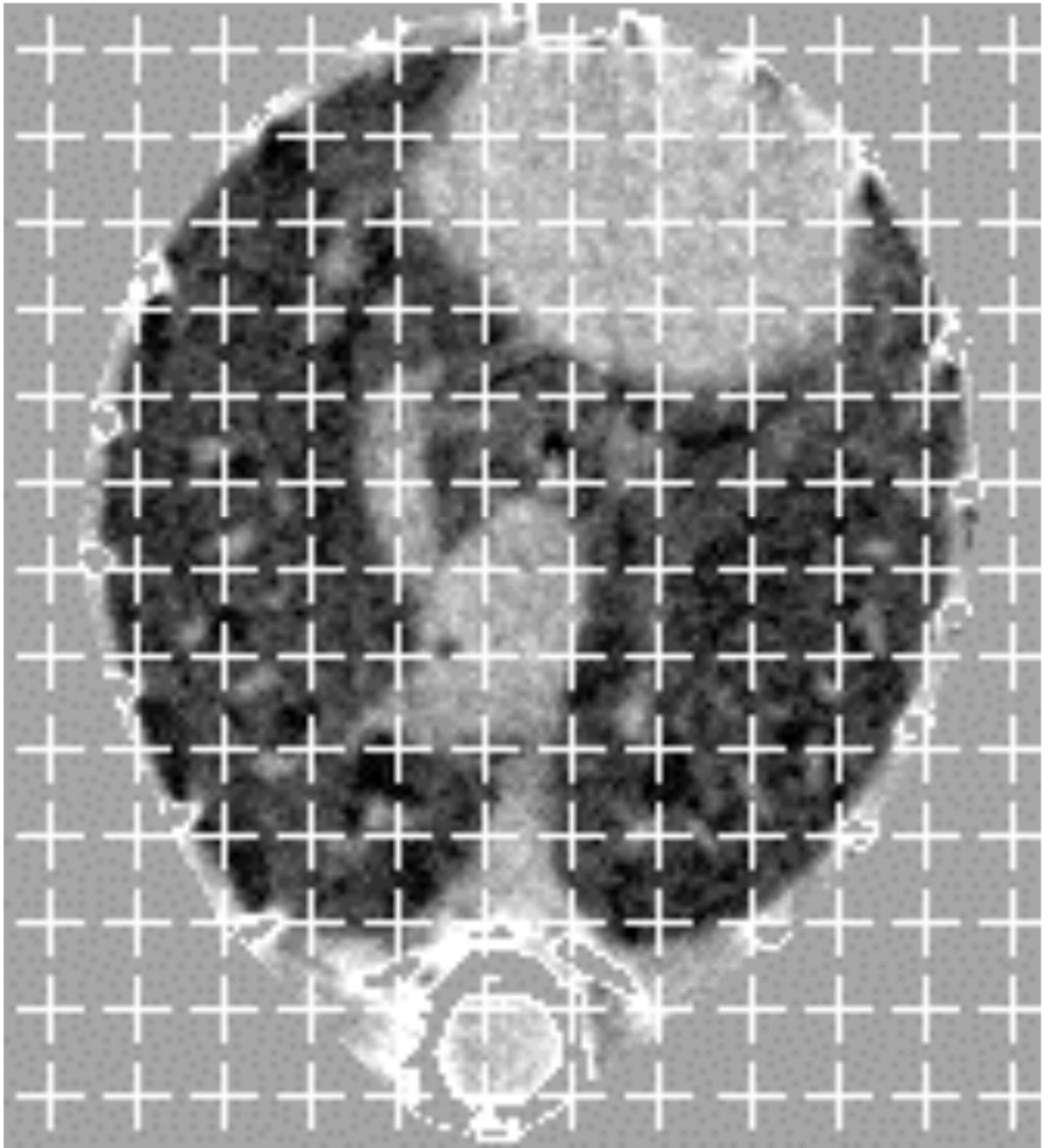


Figure 2. Axial inspiratory image of 129S6 control mouse after digital partitioning of the intrathoracic structures from the extrathoracic tissues. A point-counting grid has been overlaid for performance of Cavalieri estimation of lung volume, as described in the text.

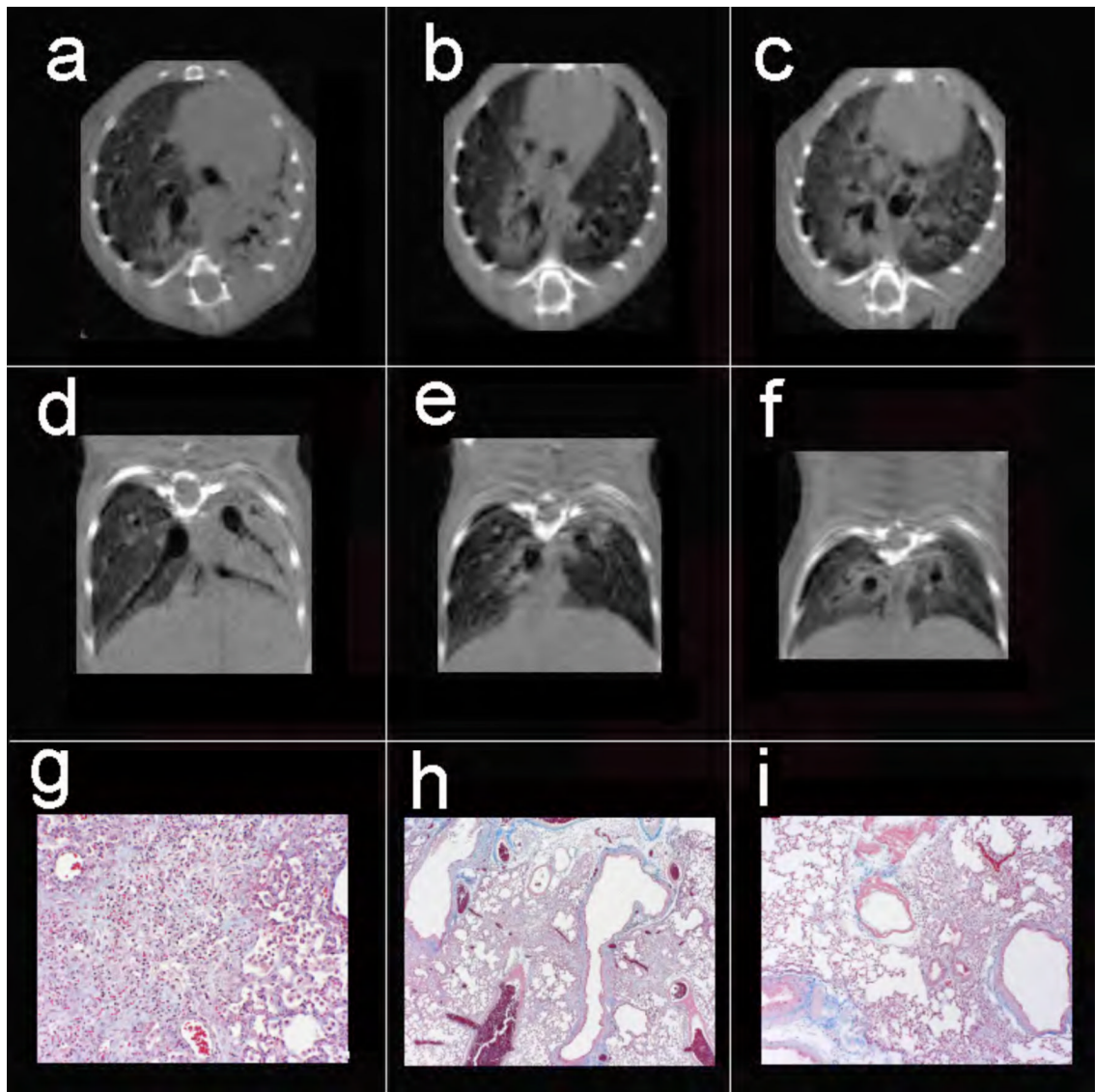


Figure 3.

Axial (a-c) and coronal (d-f) views of 3 mice exposed to 2.5, 3.0, and 3.5 U/kg bleomycin, respectively. Note the disparity in degree of injury with complete consolidation of the left lung, as well as peribronchial injury on the right in animal (a,d), focal peribronchial consolidation (b,e), and peribronchial as well as ground-glass injury (c,f). Despite the range of injury, Cqs measurements were 0.059, 0.056, and 0.056 ml/cm H₂O respectively, while Cct in the same animals were 0.074, 0.074, and 0.056 ml/cm H₂O respectively. Masson trichrome stains of the left lung from the three mice reveal diffuse confluent interstitial pneumonitis (g, 20x), peribronchial foci of interstitial pneumonitis with early fibrotic changes (h, 4x), and similar peribronchial fibrosis with adjacent normal lung (i, 20x).

Comparison of Pulmonary Compliance as Measured by microCT and Quasi-static Methods

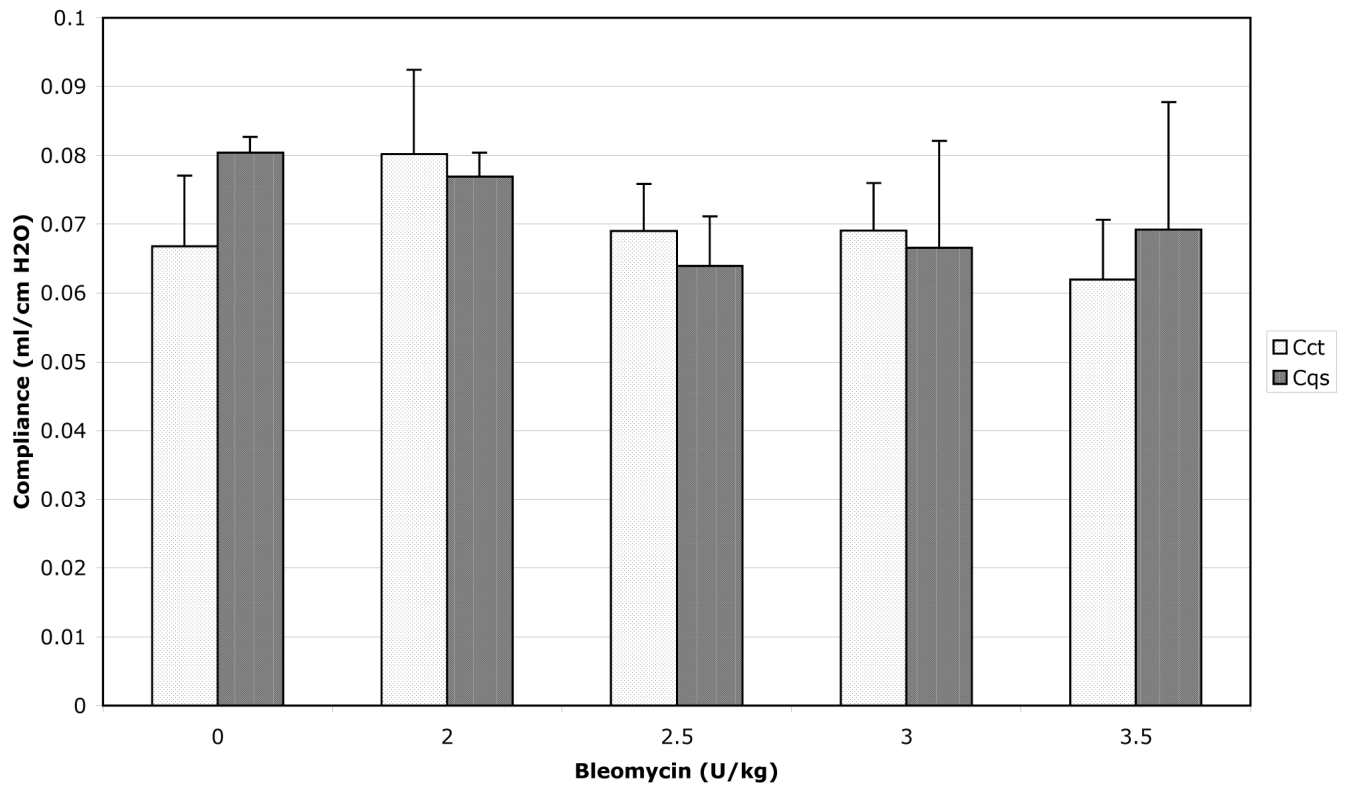


Figure 4. Comparison of quasi-static compliance measurements in 129S6/SvEv mice exposed to increasing doses of bleomycin. N = 2 mice for each pair of data points. There is no significant difference between groups (see text for details). Cct (compliance measured by microCT), Cqs (quasi-static compliance measurements), U (units).

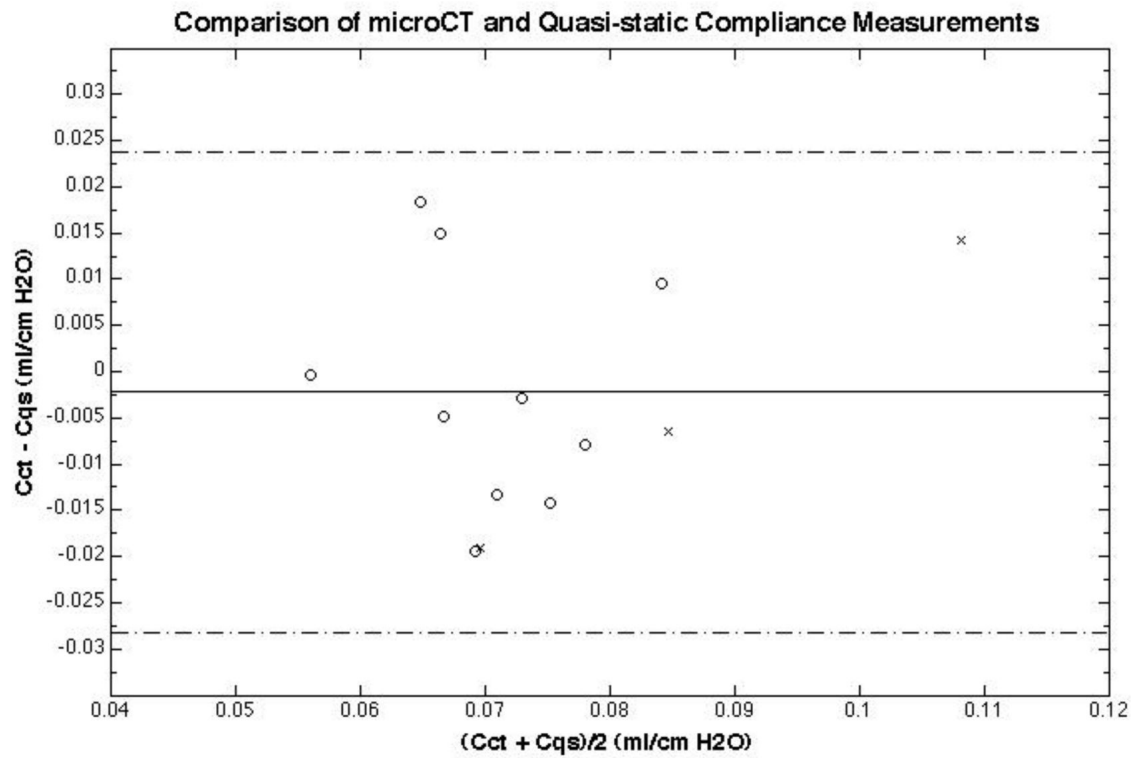


Figure 5. Bland-Altman plot showing mean compliance between Cct and Cqs vs. difference between the two measurements. The solid line is the mean difference between the two methods and the broken lines represent $\pm 2SD$. The o symbols represent all 129S6 mice exposed to saline (control animals) or bleomycin, while the + symbols C57BL6 mice with compliance measurements performed at the 3-week timepoint.

Inspiratory and expiratory lung volumes and compliance measurements in C57BL/6 mice, 1 and 3 weeks following aspiration with sterile saline

Table 1

Week	Inspiratory Vol.	Expiratory Vol.	Tidal Vol.	Cct	Cqs
1	835 ± 64	481 ± 67	354 ± 29	0.0829 ± 0.0077	
3	922 ± 217	584 ± 89	337 ± 130	0.0856 ± 0.0279	0.0894 ± 0.0110

Cct=pulmonary compliance as determined by imaging based method.

Cqs=pulmonary compliance as determined by quasi-static measurements. Mice were sacrificed following the procedure and so values are only present for the three-week timepoint.

Lung volumes are $\mu\text{l} \pm \text{SD}$ and reflect total lung volume. Compliances values are ml/cm H₂O. Differences between data points are not statistically significant.

Table 2

End-inspiratory and end-expiratory lung volumes in 129S6 mice 3 weeks following exposure to aspirated bleomycin

Bleomycin Dose (U/kg)	Inspiratory Vol.	Expiratory Vol.	Tidal Vol.
0	706 ± 18	450 ± 43	256 ± 25
2.0	832 ± 113	511 ± 64	321 ± 49
2.5	793 ± 85	510 ± 47	283 ± 38
3.0	864 ± 88	587 ± 61	276 ± 28
3.5	713 ± 60	466 ± 26	248 ± 35

N = 2 mice per group.

Inflation pressure is 8cmH₂O for each measurement as described in the text.

Inspiratory volume is the total lung volume at end-inspiration, while expiratory volume is the total lung volume at end-exhalation.

All values are in $\mu\text{l} \pm \text{SD}$ and reflect total lung volume. U=units.

Table 3

Fraction of fibrotic lung in 129S6 mice 3 weeks following exposure to aspirated bleomycin

Bleomycin Dose (U/kg)	Fibrotic Lung (%) + SD ¹
0	8.6 ± 1.5%
2.0	4.9 ± 3.4%
2.5	19.5 ± 24.8%
3.0	9.1 ± 1.5%
3.5	4.2 ± 4.5%

¹No statistical significance between groups (p = 0.698). U=units.